EPRI | ELECTRIC POWER RESEARCH INSTITUTE

How to Calculate Electric Fields to Determine Geomagnetically-Induced Currents

3002002149

How to Calculate Electric Fields to Determine Geomagnetically-Induced Currents

3002002149

Technical Update, December 2013

EPRI Project Manager

R. Lordan

ELECTRIC POWER RESEARCH INSTITUTE
3420 Hillview Avenue, Palo Alto, California 94304-1338 ▪ PO Box 10412, Palo Alto, California 94303-0813 ▪ USA
800.313.3774 ▪ 650.855.2121 ▪ askepri@epri.com ▪ www.epri.com

DISCLAIMER OF WARRANTIES AND LIMITATION OF LIABILITIES

THE FOLLOWING ORGANIZATION, UNDER CONTRACT TO EPRI, PREPARED THIS REPORT:

Natural Resources Canada

This is an EPRI Technical Update report. A Technical Update report is intended as an informal report of continuing research, a meeting, or a topical study. It is not a final EPRI technical report.

NOTE

For further information about EPRI, call the EPRI Customer Assistance Center at 800.313.3774 or e-mail askepri@epri.com.

ACKNOWLEDGMENTS

The following organization, under contract to the Electric Power Research Institute (EPRI), prepared this report:

Natural Resources Canada
580 Booth Street
Ottawa, ON

Principal Investigator
D. Boteler

This report describes research sponsored by EPRI.

This publication is a corporate document that should be cited in the literature in the following manner:

How to Calculate Electric Fields to Determine Geomagnetically-Induced Currents. EPRI, Palo Alto, CA: 2013. 3002002149.

ABSTRACT

This report describes how to calculate electric fields experienced by a power system. This calculation methodology supports determination of geomagnetically-induced currents (GICs), and is fundamental to an improved understanding of the effect of geomagnetic disturbances (GMDs) on power systems. The electric field calculation method collects input data about the Earth's conductivity structure, as well as magnetic field data or electrojet information. The report first presents the theoretical fundamentals on which the electric field calculations are based. It then demonstrates that different frequencies penetrate to different depths within the Earth, thus requiring knowledge of the conductivity down into the crust and mantle. This information can be used to calculate the "plane wave" surface impedance for a multi-layer model of the Earth. The report then shows how the source characteristics can be included in the induction calculations and yield expressions for the electric field produced by the auroral electrojet.

Keywords
Auroral electrojet
Earth conductivity
Geoelectric field
Geomagnetic disturbances, GMDs
Geomagnetically-induced currents, GICs
Surface impedance

CONTENTS

LIST OF FIGURES

1
INTRODUCTION

As part of assessing the geomagnetic effects on power systems, it is necessary to be able to calculate the geomagnetically-induced currents (GIC) that will flow in a power system. This involves calculation of the electric fields experienced by the power system and using them as input to a network model to calculate the GIC, as shown in Figure 1-1. This report is concerned with the first part of this problem: calculating the electric fields given information about the Earth conductivity structure and using either magnetic field data or electrojet information as input.

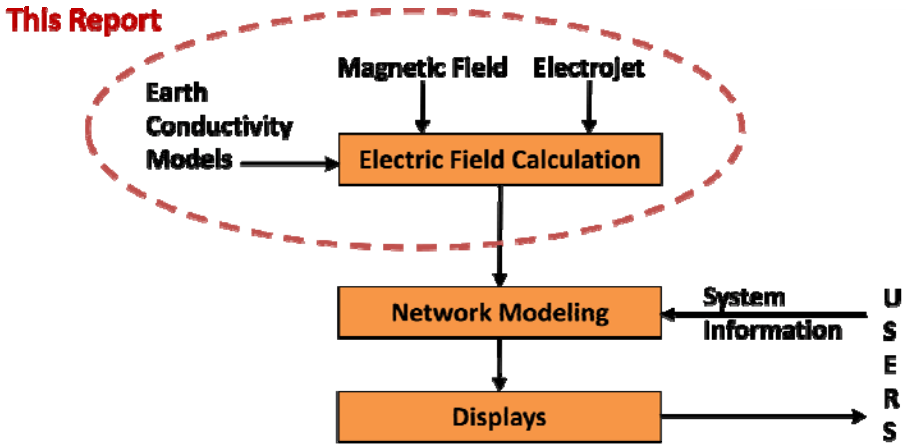

Figure 1–1
Calculation of geomagnetic impact on power systems: calculation of electric fields

To start, we present the theoretical fundamentals on which the electric field calculations are based. From this it is shown that different frequencies penetrate to different depths within the Earth and requires knowledge of the conductivity down into the crust and mantle. This can be used to calculate the "plane wave" surface impedance for a multi-layer model of the Earth. It is then shown how the source characteristics can be included in the induction calculations and give expressions for the electric field produced by the auroral electrojet.

2
THEORETICAL FUNDAMENTALS

The starting point, as with any electromagnetic problem, is Maxwell's equations. For subsequent use we start with the differential forms

$$\nabla x H = J + \frac{\partial D}{\partial t} \quad \text{Eq. 2-1}$$

$$\nabla x E = -\frac{\partial B}{\partial t} \quad \text{Eq. 2-2}$$

$$\nabla . D = \rho \quad \text{Eq. 2-3}$$

$$\nabla . B = 0 \quad \text{Eq. 2-4}$$

Equation 2-1 is Ampere's law expressing the magnetic field strength H produced by a current J and displacement current $\partial D/\partial t$. Equation 2-2 is Faraday's law relating the curl of the electric field, E, to the rate of change of the magnetic flux density B. Equation 2-3 describes the divergence of the electric flux density, D, due to a charge density, ρ, and Equation 2-4 expresses the non-divergent nature of the magnetic field.

We also need the constitutive relations

$$J = \sigma E \qquad B = \mu H \qquad D = \varepsilon E \quad \text{Eq. 2-5}$$

showing how the fields are related by the properties of the medium: conductivity, σ, magnetic permeability, μ, and permittivity, ε (also called the dielectric constant).

Assuming a time variation of the form e^{iwt} we can write $\frac{\partial B}{\partial t} = Be^{iwt}$. Making this substitution and using the constitutive relations we can rewrite Equations 2-1 and 2-2 as

$$\nabla x H = \sigma E + i\omega\varepsilon E \quad \text{Eq. 2-6}$$

$$\nabla x E = i\omega\mu H \quad \text{Eq. 2-7}$$

Taking the curl of Equation 2-7 gives

$$\nabla x(\nabla x E) = i\omega\mu(\nabla x H) = (i\omega\mu\sigma - \omega^2\varepsilon\mu)E \quad \text{Eq. 2-8}$$

For regions with no free charge, $\nabla . E = 0$, and then Equation 2-8 can be written

$$\nabla^2 E = (i\omega\mu\sigma - \omega^2\varepsilon\mu)E \quad \text{Eq. 2-9}$$

This is the general equation for wave propagation in a conducting medium [1]. In the case where the conductivity, σ, is zero, the first term in brackets on the right-hand side of Equation 2-9 can be dropped, giving

$$\nabla^2 E = -\omega^2\varepsilon\mu E \quad \text{Eq. 2-10}$$

which is the equation for wave propagation in a vacuum.

Under the condition that $\sigma \gg \omega\varepsilon$, i.e. for low frequencies in a conducting medium, then the second term in brackets on the right-hand side of Equation 2-9 can be dropped giving

$$\nabla^2 E = i\omega\mu\sigma E \qquad \textbf{Eq. 2-11}$$

which is the diffusion equation for the electric fields in the conducting medium. The same form as Equations 2-10 and 2-11 can also be derived for the magnetic fields.

It will be seen in the next section that geomagnetic induction at the frequencies of concern for GIC (0.001 to 1 Hz) satisfies the condition for the diffusion equation. This corresponds to ignoring the "displacement current" term in Equation 2-1. This is sometimes referred to as "quasi-static induction." This approach has been used by such developers of geomagnetic induction theory as Price [2] and Weaver [3]. Their approach is preferred here as it allows for a completely general specification of the source magnetic field variations responsible for GIC. The magnetic field structure can then be defined to correspond to particular types of geomagnetic field variation, e.g. magnetic substorms, storm sudden commencement (SSC), etc.

Early development of geomagnetic induction theory was strongly influenced by the theory for electromagnetic wave propagation. In his pioneering paper, Cagniard considered the source as a plane electromagnetic wave normally incident on the Earth's surface [4]. Weaver puts this approach in perspective, saying:

"While this approach certainly leads to correct results for the field on and within the Earth, it also conveys, unfortunately, a rather misleading physical picture of the induction phenomenon. For example the wavelength of a field oscillating with the relatively high frequency (within the spectrum of geomagnetic variations) of 1 Hz is almost 50 earth radii, while the longer period substorm variations have wavelengths about 10^7 times the height of their ionospheric source currents! It does not seem particularly helpful to imagine a plane electromagnetic wave propagating downwards from the ionosphere under such circumstances; the earth's surface is very definitely in the near field of the source - plane waves belong to the far field." [3]

In spite of Weaver's comments, such terms as "plane wave method" or "plane wave impedance" can be found sprinkled throughout the literature. Although such terms may be considered inappropriate, closer inspection shows that the theoretical developments in such papers are correctly based on the diffusion equation. This can be shown by expanding the first term in Equation 2-11 to give

$$\frac{\partial^2 E}{\partial x^2} + \frac{\partial^2 E}{\partial y^2} + \frac{\partial^2 E}{\partial z^2} = i\omega\mu\sigma E \qquad \textbf{Eq. 2-12}$$

In cases where the source magnetic field is very broad, then the variation with x and y is negligible and the first two terms of Equation 2-12 can be dropped, resulting in the equation

$$\frac{\partial^2 E}{\partial z^2} = i\omega\mu\sigma E \qquad \textbf{Eq. 2-13}$$

This has the solution

$$E = E_0 e^{-z/p} \qquad \textbf{Eq. 2-14}$$

where $p = 1/\sqrt{i\omega\mu\sigma}$ is the complex skin depth. The fall-off of the electric field amplitude is given by the real part

$$\delta = \sqrt{\frac{2}{\omega\mu\sigma}} \qquad \text{Eq. 2-15}$$

Substituting into Equation 2-7 gives

$$\sqrt{i\omega\mu\sigma}E = i\omega\mu H \qquad \text{Eq. 2-16}$$

which, with rearranging, gives

$$\frac{E}{H} = \sqrt{\frac{i\omega\mu}{\sigma}} \qquad \text{Eq. 2-17}$$

This is termed the “surface impedance” and gives the relation between the electric and magnetic fields at the surface of a uniform half-space. It will be shown later that expressions for the surface impedance can also be derived for a multi-layer model that represents the change of conductivity with depth within the Earth.

For geomagnetic induction, these expressions are valid for conditions where the horizontal scales of the source fields are large compared to the skin depths in the Earth. This condition is upheld for a range of situations in geomagnetic induction studies, so these expressions are very useful in practice. However, for localized source fields, such as due to an auroral electrojet, it is necessary to take into account the horizontal variations of the fields. It is therefore useful to distinguish the results such as in Equation 2-17 from these more general cases. It could be argued that they should be called “surface impedance for the condition where the horizontal variations are considerably smaller than the vertical variations,” but “plane wave surface impedance” somehow caught on. There is nothing wrong in this as long as, remembering Weaver's comments above, the term is not taken literally and is just used as a shorthand to identify the solutions of the diffusion equation where the horizontal scales are much larger than the skin depth.

3
SKIN DEPTH IN THE EARTH

During geomagnetic disturbances the variations of the magnetic field induce electric fields that drive electric currents in the Earth and in conductors at the Earth's surface. The electric currents induced in the Earth themselves create a magnetic field that adds to the magnetic field variation observed at the Earth's surface. Thus the observed magnetic field comprises two parts: that due to external currents in the ionosphere and magnetosphere; and that due to the internal currents in the Earth. The "internal" magnetic field is such that it tends to cancel the "external" magnetic field so that the total magnetic field variation falls off with increasing depth within the Earth. The induced currents in the Earth fall-off at the same rate as the magnetic field variation. In a uniform medium, the fields have an exponential fall-off characterized by the skin depth, δ, given by Equation 2-15.

In a non-uniform Earth the fall-off in each layer depends on the conductivity of that layer, and the penetration of the magnetic field depends on the combined effect of all the layers. In high conductivity regions larger induced currents can flow, resulting in a greater cancelling of the external magnetic field and so producing a smaller skin depth than in low conductivity areas. Also, the skin depth dependence on frequency means that low frequency variations penetrate much deeper into the Earth than higher frequency variations. This is illustrated in Figure 3-1. At the frequencies that are significant for GIC in power systems (1 Hz down to 0.0001 Hz) the skin depths range from kilometers to hundreds of kilometers and it is necessary to take into account the earth conductivity down to these depths.

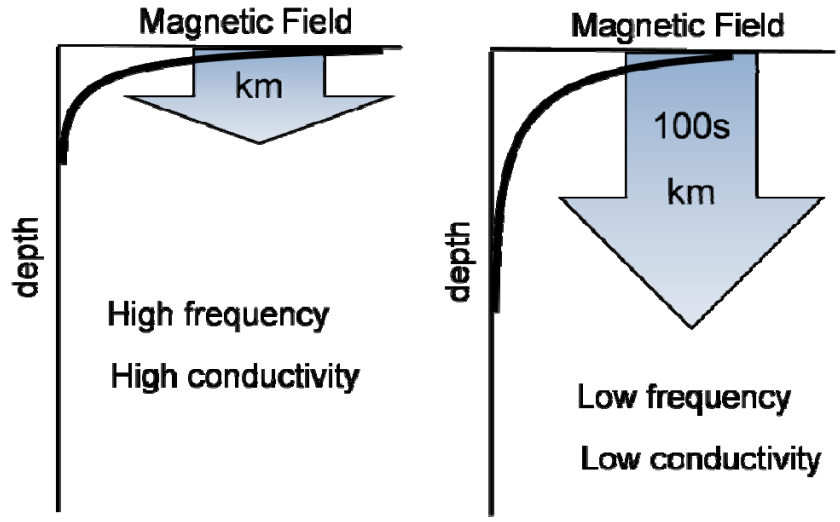

Figure 3–1
Skin depths in the Earth for different conductivities and frequencies

4
EARTH CONDUCTIVITY STRUCTURE

The Earth is comprised of a thin crust, up to 62 miles (100 km) thick, above the mantle. Below that is the core comprising an outer liquid core around a solid inner core as shown in Figure 4-1.

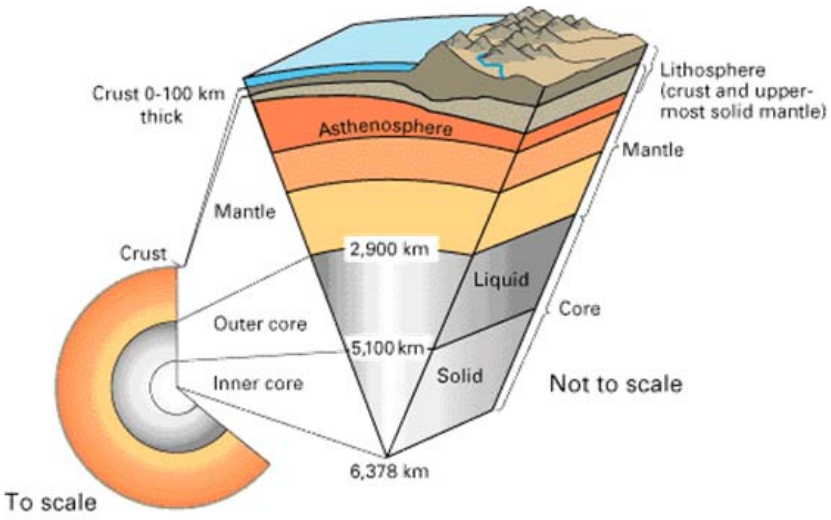

Figure 4–1
Schematic of the interior structure of the Earth

At the surface of the Earth there is considerable variation in the conductivities of different regions. Igneous rocks at the core of continental blocks, such as the Canadian Shield, have low conductivities, while sedimentary rocks have a higher conductivity. The even higher conductivity of seawater can also have an influence on the electric fields on land near the coast. Deeper in the Earth the crust has a generally low conductivity, while below that in the mantle the increasing pressure and temperature lead to higher conductivities. Figure 4-2 shows examples of Earth models for different parts of North America.

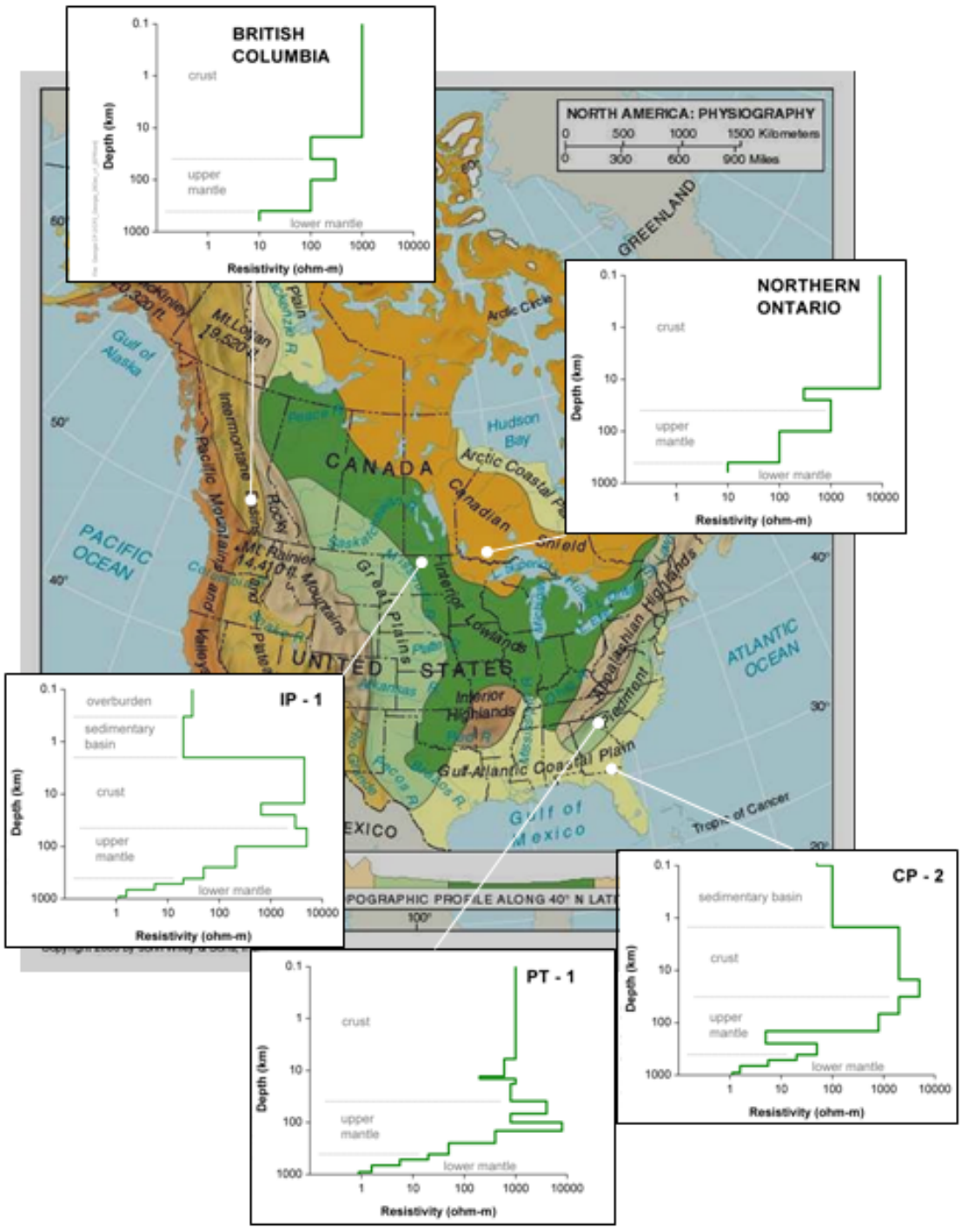

Figure 4–2
Map showing geological regions of North America with insets showing the conductivity variation with depth in selected regions

5
CALCULATION OF SURFACE IMPEDANCE

A simple layered-Earth model, such as in Figure 5-1, can be used to represent the change of conductivity with depth within the Earth.

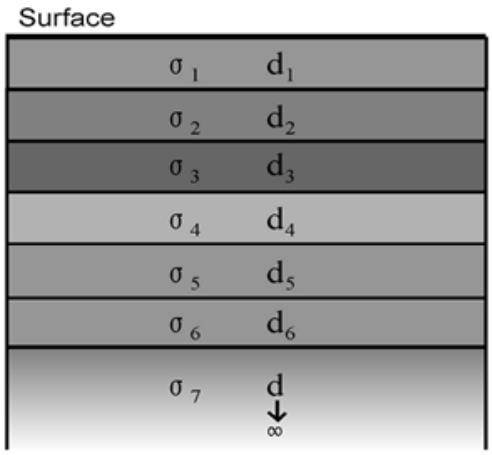

Figure 5–1
Multi-layer model of the Earth

The impedance at the surface can be calculated using recursive relations in a manner analogous to transmission line theory. Each layer is characterized by its propagation constant

$$k_n = \sqrt{i\omega\mu\sigma_n} \qquad \textbf{Eq. 5-1}$$

The impedance at the surface of the bottom layer is then given by

$$Z_n = \frac{i\omega\mu}{k_n} \qquad \textbf{Eq. 5-2}$$

This is then used to calculate the reflection coefficient seen by the layer above

$$r_n = \frac{1 - k_n \frac{Z_{n-1}}{i\omega\mu}}{1 + k_n \frac{Z_{n-1}}{i\omega\mu}} \qquad \textbf{Eq. 5-3}$$

This can then be used to calculate the impedance at the top surface of that layer

$$Z_n = i\omega\mu\left(\frac{1 - r_n e^{-2k_n d_n}}{k_n\left(1 + r_n e^{-2k_n d_n}\right)}\right) \qquad \textbf{Eq. 5-4}$$

These steps are then repeated for each layer up to the surface.

The propagation constants and hence the resulting impedances are functions of frequency, so this sequence of calculations has to be repeated for each frequency that will be needed for calculating the electric fields. The exact frequencies will depend on the sampling rate of the magnetic data and the duration of the data used, as will be shown in the next section.

The final set of surface impedance values represents the transfer function of the Earth to be used in the calculations of the electric fields.

6
PRACTICAL CALCULATIONS USING MAGNETIC FIELD DATA

Because of the frequency dependence of the Earth surface impedance, it is easier to make the calculations in the frequency domain. The sequence of operations is shown in Figure 6-1. Starting with a time series of magnetic field values, a Fast Fourier Transform (FFT) is used to obtain the frequency spectrum of the magnetic field variations. The magnetic field spectral value at each frequency is then multiplied by the corresponding surface impedance value to obtain the electric field spectral value. This then gives the frequency spectrum of the electric field. An inverse FFT is then used to obtain the electric field values in the time domain.

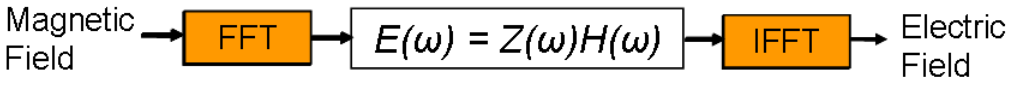

Figure 6–1
Using magnetic data to calculate electric fields

An example of the frequency domain parameters is shown in Figure 6-2. This shows the magnetic field spectrum for Ottawa and calculated electric field spectrum and the surface impedance for Quebec. The magnetic field data and calculated electric fields in the time domain are shown in Figure 6-3.

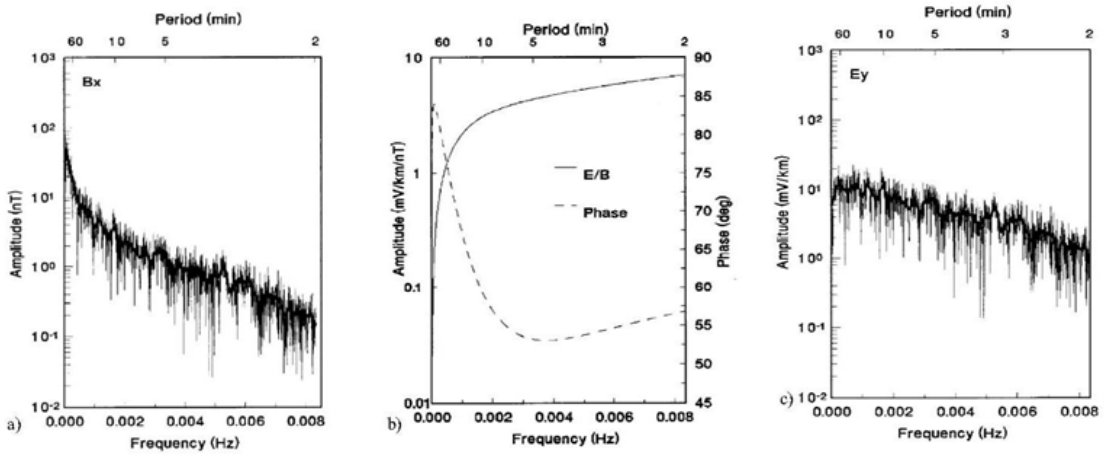

Figure 6–2
Frequency domain parameters in electric field calculations: a) magnetic field spectrum, b) surface impedance, and c) electric field spectrum

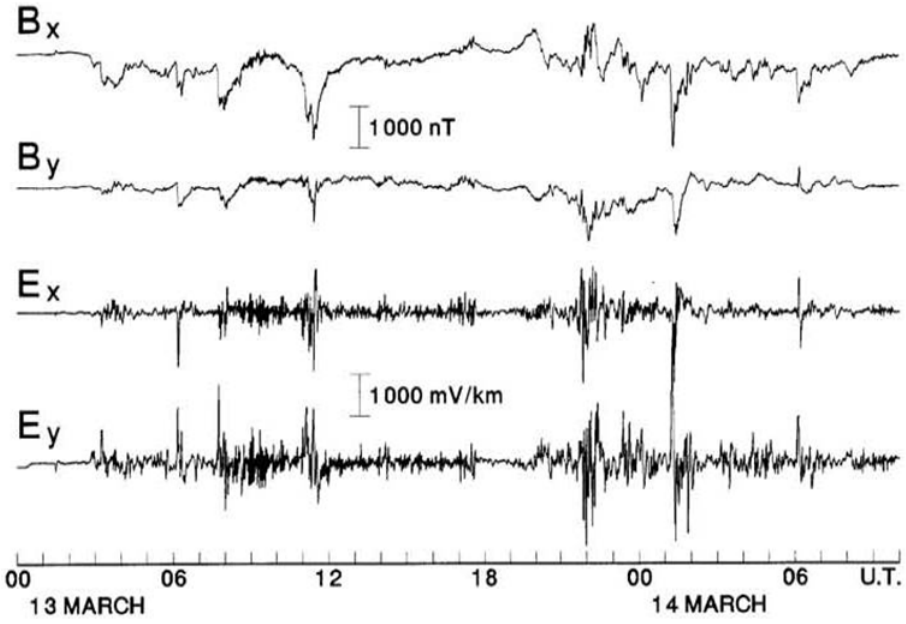

Figure 6–3
Recordings at the Ottawa Magnetic Observatory on March 13-14, 1989, of the northward (B_x) and eastward (B_y) components of the magnetic field and the calculated northward (E_x) and eastward (E_y) electric fields

The detailed steps in the calculations are as follows:

Choose the magnetic data to use and note the sampling interval, Δt, and the duration, T.

Fast Fourier Transforms work more efficiently with data that is a series of N values where N is a power of 2. One day of magnetic data sampled every minute gives 1440 values. This can have zeros added to give a time series of 2048 points, or a data set of 2048 values used which extends the magnetic data into the following day (as in Figure 6-4).

Precondition the magnetic data time series. This involves removing the mean from the set of data. Also remove any linear trend in the data. These two steps can be combined by taking the average of the first 60 values to give an average value, A, for the start of the time series and the average of the last 60 values to give an average value, B, for the end of the time series. For each value in the time series from i = 1 to i = N, subtract the "trend" value
$C(i) = A(N - i) / N + Bi / N$.

Tapering of the magnetic data time series. The ends of the data series can introduce steps in the analyzed time series that produce spurious effects in the frequency spectrum. To avoid this it is necessary to taper the end of the time series. This can be done by multiplying the end 60 values by a "cosine-bell" given by:

$$w_p(t) = \begin{cases} \frac{1}{2}(1 - cos 2\pi t/p), & 0 \le t < p/2 , \\ 1, & p/2 \le t < 1 - p/2 , \\ \frac{1}{2}(1 - cos 2\pi t/p), & 1 - p/2 \le t \le 1 \end{cases} \qquad \text{Eq. 6-1}$$

Convert to complex numbers. Many FFT routines expect the input data to be an array of complex numbers. The magnetic time series data, BB(i), is real but can be converted to complex values CC(i) with imaginary parts equal to zero.

The time series is now ready for performing the Fourier transform. Many analysis packages have a built-in Fourier transform routine that can be used. Alternatively there are routines for C and Fortran in the *Numerical Recipes* books [5]. Many other algorithms for performing the Fast Fourier Transform are available in the literature and in computing libraries. All of them perform essentially the same function.

For a time series of N data samples with a sampling interval Δt (hence having a duration $T = N.\Delta t$), the FFT will produce an array of complex values as the same size as the input array. (Some routines overwrite the input array, so the input data should be stored in a separate array if it is to used later, for example in plotting the results.) The output array contains values at positive and negative frequencies $f_i = i / N\Delta t$ for $i = 1$ to $N/2$. The input is N real values (i.e., N pieces of information), while the output is N complex values so would appear to have 2N pieces of information. However, the values at negative frequencies are the complex conjugate of the values at positive frequencies, and so contain no new information; therefore we have N pieces of information in the output.

We normally plot negative frequencies to the left, positive frequencies to the right, with zero frequency in the middle, as shown in Figure 6-4 (a). However, FFTs often produce an output array with the positive frequencies first and the negative frequencies appended at the end of the array, as shown in Figure 6-4 (b).

The FFT produces values at the frequencies $0, \pm f_1, \pm 2f_1, \pm 3f_1, \pm 4f_1, \ldots \pm(N-1)/2f_1, (N/2)f_1$.

Where $f_1 = 1/N\Delta t$. These are the frequencies for which the surface impedance must be calculated. For each of these frequencies, multiply the magnetic field spectral value by the surface impedance to give the corresponding electric field spectral value. It is worthwhile checking that the electric field negative frequency values are the complex conjugate of the positive frequency values. The correct result in the time domain will not be obtained if this is not the case.

Now perform an inverse FFT on the electric field spectrum. This will give an array of complex values that contains the electric field in the time domain. Just as with the original magnetic field data, the electric field data must be real. Thus the computed array of electric field values should comprise complex values for which the imaginary parts are all zero. This should be checked as a test that the calculations have been made correctly.

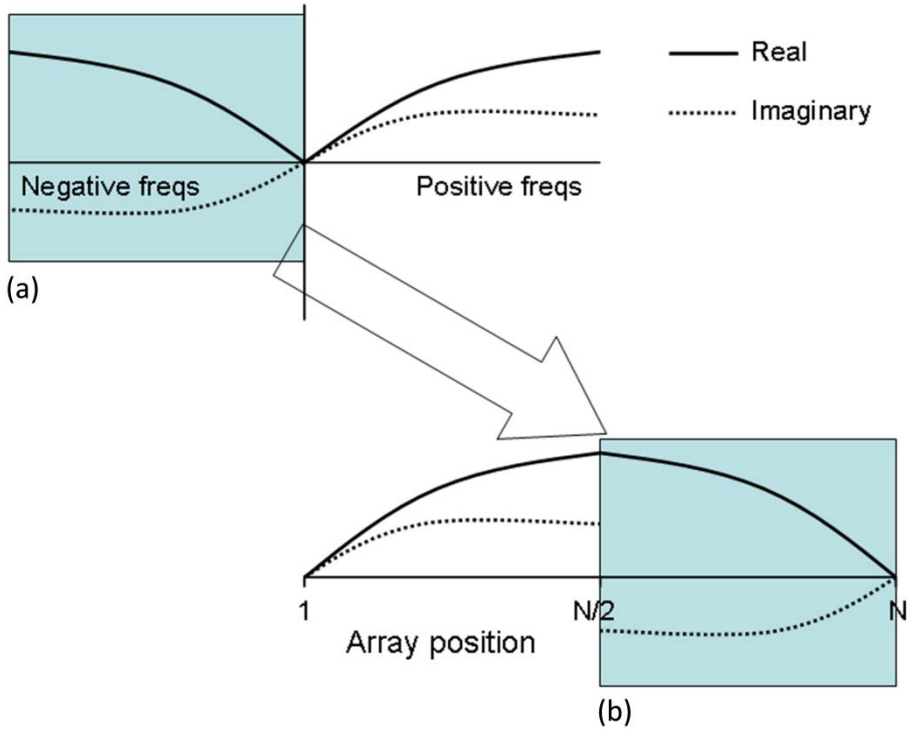

Figure 6–4
Spectral values at the negative frequency are output at end of array

7
CALCULATIONS FOR AN AURORAL ELECTROJET SOURCE

The above calculations use the assumption that the magnetic field variations are uniform across the area of the power system. In practice the disturbance fields are not uniform. For example, the auroral electrojet is the cause of magnetic substorms that are responsible for the largest GICs in power systems. The magnetic and electric fields produced by the auroral electrojet can be calculated using the complex image method in the same way as calculations are made of electromagnetic coupling between adjacent transmission lines (Figure 7-1).

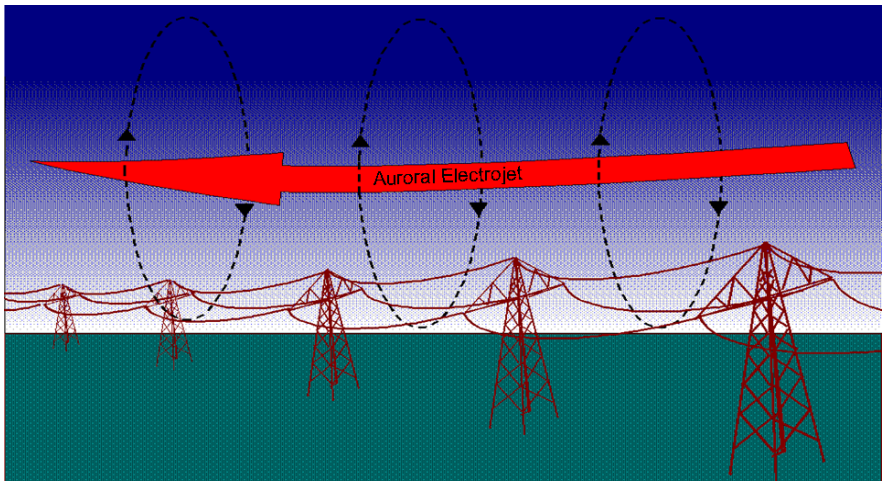

Figure 7–1
Electromagnetic coupling between the auroral electrojet and power transmission lines

First we will show the calculations by assuming that the electrojet can be considered as a line current at a height of 62 miles (100 km). Later we will show how the complex image method can be extended to include the width of the electrojet.

Figure 7-3 shows a line current at a height, h, above the Earth's surface. The total variation fields at the Earth's surface are due, as mentioned earlier, to the field of the external source plus the field due to the currents induced in the Earth. The exact calculation of the fields due to the induced currents requires expressing the fields in terms of the wavenumber components of the source and integration over all wavenumbers. However, it has been shown that the “internal” fields are approximated, to good accuracy, by the fields due to an image current at a complex depth. This means that the complex skin depth, p, can be represented as a reflecting surface so that the image current is the same distance below this level as the source current is above (Figure 7-2). The magnetic and electric fields are then given by the source and image currents and their distances from the location on the surface as shown in Figure 7-2.

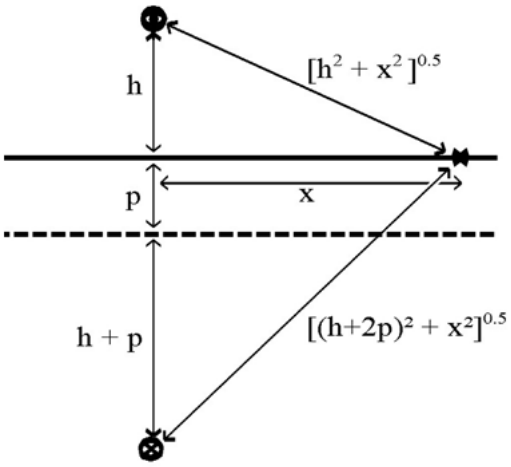

Figure 7–2
Complex image method

The magnetic and electric fields at horizontal distance from the source current are then given by

$$B_x = \frac{\mu_0 I}{2\pi}\left(\frac{h}{h^2+x^2} + \frac{h+2p}{(h+2p)^2+x^2}\right) \quad \textbf{Eq. 7-1}$$

$$B_z = -\frac{\mu_0 I}{2\pi}\left(\frac{x}{h^2+x^2} - \frac{x}{(h+2p)^2+x^2}\right) \quad \textbf{Eq. 7-2}$$

$$E_y = -\frac{j\omega\mu_0 I}{2\pi} \ln\left(\frac{\sqrt{(h+2p)^2+x^2}}{\sqrt{h^2+x^2}}\right) \quad \textbf{Eq. 7-3}$$

where the complex skin depth is related to the surface impedance by the expression

$$p = \frac{Z_s}{j\omega\mu} \quad \textbf{Eq. 7-4}$$

In practice the auroral electrojet spreads over about 6 degrees of latitude. The current profile is difficult to determine, but the studies that have been made show that it can vary considerably. In practice, without special studies for each event, we cannot specify the current profile of the electrojet. However, to improve on the simple line current model and to include a simple approximation to the width of the electrojet, we can represent the electrojet current profile by a Cauchy distribution as shown in Figure 7-3 (b). It has been shown that the fields produced by this current profile with a half-width ‘a’ at a height ‘h’ are the same as the fields produced by a line current at a height ‘h+a’. Figure 7-3 (a) shows a Cauchy distribution current profile with a half width of 124 miles (200 km) at a height of 62 miles (100 km) and the equivalent line current at a height of 186 miles (300 km).

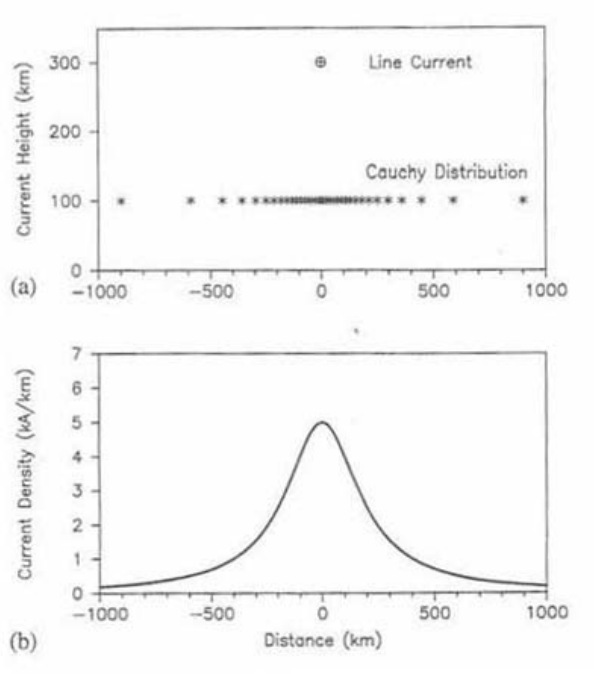

Figure 7–3
Cauchy distribution representation of an auroral electrojet and the equivalent line current at a height h+a

The fields of the wide electrojet can then be calculated using the equivalent line current at a greater height and the corresponding image current using the formulas:

$$B_x = \frac{\mu_0 I}{2\pi}\left(\frac{h+a}{(h+a)^2+x^2} + \frac{h+a+2p}{(h+a+2p)^2+x^2}\right) \quad \textbf{Eq. 7-5}$$

$$B_z = -\frac{\mu_0 I}{2\pi}\left(\frac{x}{(h+a)^2+x^2} - \frac{x}{(h+a+2p)^2+x^2}\right) \quad \textbf{Eq. 7-6}$$

$$E_y = -\frac{j\omega\mu_0 I}{2\pi} \ln\left(\frac{\sqrt{(h+a+2p)^2+x^2}}{\sqrt{(h+a)^2+x^2}}\right) \quad \textbf{Eq. 7-7}$$

Calculations made using the above formulas for an electrojet of 1 million amperes with a half-width of 124 miles (200 km) at a height of 62 miles (100 km) varying with a period of 5 minutes give the magnetic and electric fields shown in Figure 7-4.

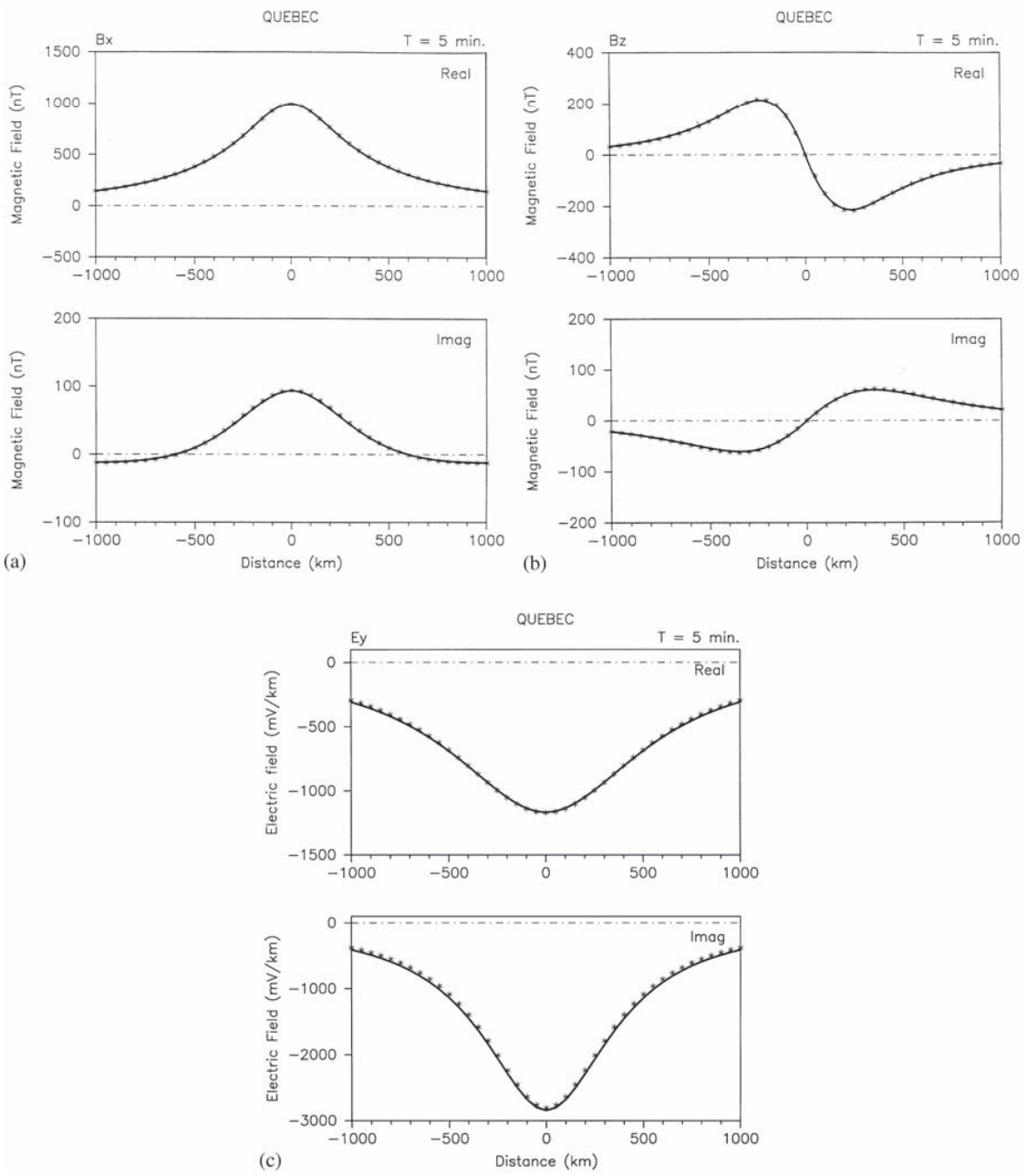

Figure 7–4
Magnetic and electric fields produced by a "wide" electrojet. Asterisks show the results of calculations made using the complex image method. Solid lines show results for the exact expressions obtained by numerical integration.

These electric fields can be used as input into a power system model to calculate the GIC that would be produced by an electrojet at a specified location relative to the power system.

8
REFERENCES

1. Jordan, E.C. and Balmain, K.G. *Electromagnetic Waves and Radiating Systems*. Second edition, Prentice-Hall, Englewood Cliffs, N.J. 1968, p. 753.
2. Price, A.T., "The Theory of Magnetotelluric Methods When the Source Field is Considered." *Journal of Geophysical Research*. Vol. 67, No. 5, pp. 1907-1918 (1962).
3. Weaver, J.T. *Mathematical Methods for Geo-electromagnetic Induction.* Research Studies Press, Taunton, N.J. 1994, p. 316.
4. Cagniard, L., "Basic Theory of the Magnetotelluric Method of Geophysical Prospecting," *Geophysics*. Vol. 18, No. 3, pp. 605-635 (1953).
5. Press, W.H., Teukolsky, S.A., Vetterling, W.T., and Flannery, B.P. *Numerical Recipes in Fortran: The Art of Scientific Computing*. Second edition, Cambridge University Press, Cambridge, England 1992.

The Electric Power Research Institute, Inc. (EPRI, www.epri.com) conducts research and development relating to the generation, delivery and use of electricity for the benefit of the public. An independent, nonprofit organization, EPRI brings together its scientists and engineers as well as experts from academia and industry to help address challenges in electricity, including reliability, efficiency, affordability, health, safety and the environment. EPRI also provides technology, policy and economic analyses to drive long-range research and development planning, and supports research in emerging technologies. EPRI's members represent approximately 90 percent of the electricity generated and delivered in the United States, and international participation extends to more than 30 countries. EPRI's principal offices and laboratories are located in Palo Alto, Calif.; Charlotte, N.C.; Knoxville, Tenn.; and Lenox, Mass.

Together…Shaping the Future of Electricity

3002002149

Electric Power Research Institute
3420 Hillview Avenue, Palo Alto, California 94304-1338 • PO Box 10412, Palo Alto, California 94303-0813 • USA
800.313.3774 • 650.855.2121 • askepri@epri.com • www.epri.com